UNIVERSITA' DEGLI STUDI DI GENOVA

Corso di Dottorato di ricerca in

SCIENZE PEDIATRICHE

Curriculum: PATOLOGIA FETO-PERINATALE E PEDIATRICA

"IMMUNOHISTOCHEMICAL CHARACTERIZATION OF A SERIES OF PEDIATRIC MEDULLOBLASTOMAS"

Investigation of JAM molecules expression in pediatric medulloblastoma

Tutor:

Chiar. mo Prof. Ezio Fulcheri

Ph.D candidate:

Dott.ssa Chiara Baldovini

Abstract

Background and aims. Medulloblastoma (MB) is the most frequent embryonal tumor of the CNS and the most common malignat pediatric brain tumor, arising mainly in the fourth ventricle. MB is characterized by four molecularly defined subgroups with distinct clinicopathological features and prognosis: WNT (MB^{WNT}), SHH (MB^{SHH}), group 3 (MB^{Grp3}), and group 4 (MB^{Grp4}). Standard therapy is ineffective in subsets of MB, thus there is a great need to identify novel prognostic markers and treatment targets. Junctional adhesion molecules (JAM)-A, -B, -C may be relevant candidate for this role, based on clinical and preclinical data. The aim of this study was to examine gene and protein expression of JAMs and assess their prognostic value by relying on both open access large datasets and a sample of pediatric MB.

Methods. In the gene expression study, founded on two public datasets (n=763 and n=223), combined risk stratification models based on transcript levels of JAM genes (namely F11R, JAM-2 and JAM-3) and clinically relevant features were identified by multivariate Cox proportional hazards analysis. In the experimental study, we sought to examine the immunohistochemical expression of JAM-A,B,C in a sample of pediatric MB (n=65). Nanostring profiling and immunohistochemistry were adopted to obtain molecular classification. Association and survival analyses were conducted to validate trascriptomic findings.

Results. Gene expression analyses showed that JAMs were differentially expressed across consensus molecular subgroups of MB ($p<0.0001$). In particular, JAM-3 was differentially expressed between MB^{Grp3} and MB^{Grp4} and its overexpression was significantly associated with large cell/anaplastic (LC/A) pathology (p=0,007) and shorter survival (p=0,002). These findings were only partially supported by immunohistochemical data, since high expression (3+) of JAM-C was strongly associated with a subset of MB^{Grp3} with LC/A pathology but did not differentiate between MB^{Grp3} and MB^{Grp4}. Further, survival analyses displayed a trend for a shorter survival in patients with high expression of JAM-C. Thus, JAM-C may be useful to identify a subset of MB^{Grp3} with LC/A pathology carrying poor clinical outcomes.

Conclusions. JAM-C may have a role as subtyping marker and prognostic factor in pediatric MB. Our findings are consistent with recent evidence suggesting that MB^{Grp3} and MB^{Grp4} display significant molecular overlap. In particular, JAM-C is useful to identify a subset of MB^{Grp3} showing LC/A pathology and dismal prognosis which could at least partially correspond to a recently identified high-risk subtype of MB^{Grp3} showing LC/A pathology and harbouring MYC amplification. Given the lack of reliable immunohistochemical markers for such emerging subgroup, further studies are needed to investigate the role of JAM-C in relation to clinicopathological features, molecular characteristics and overall prognosis.

1. Introduction

Background

1.1 Epidemiology

Medulloblastoma (MB) is the most common embryonal tumor of the CNS and the most common malignat pediatric brain tumor, arising mainly in the fourth ventricle [1]. The overall incidence of MB is estimated ranging from 2,34 to 5,96 per 1 million population and has not changed over time [1, 2]. Despite being considered a pediatric malignancy, up to a quarter of all MB occur among adult population; however, taken together these cases represent less than 1% of all brain tumors.

1.2 Clinical presentation

Clinical presentation includes mainly sings of raised intracranial pressure, such as headache, nausea upon waking and vomiting; less frequently, tumor growth is revealed by compression of anatomic structures located in the brain stem.

1.3 Risk stratification and treatment: the standard of care

The workup of risk stratification among “average-risk” and “high-risk” disease has been based for years on few primary criteria, including age, extent of surgery, metastatic spread and histological variant [3]. In most cases, maximal surgical excision is the first therapeutic approach. Patients with average-risk disease receive craniopinal radiotherapy with or without chemotherapy. For high-risk disease, craniospinal radiotherapy is administred at a higher dose, followed by chemotherapy. In selected cases, stem cell transplant is also considered before chemotherapy. The current standard of care leads to encouraging results, with an estimated rate of cure of approximately 70% [4]. Nonetheless, patients with metastatic disease have poor outcomes, with 5-year survival rate of less than 40%. Moreover, long-term survivors – especially infants and those patients exposed to higher dose - often experience considerable treatment-related side effects such as neurocognitive and neuroendocrine disorders, hearing loss and secondary benign and malignant tumors [5].

1.4 The integrated diagnosis

In the last decade, the identification of clinically relevant molecular subgroups of MB has given a major contribution to risk assessment. Thus indeed, unsupervised hierachical clustering analyses applied to transcriptome, microRNA and methylome profiling obtained from multi-institutional cohorts of MB highlighted 4 subgroups of disease: WNT (MB^{WNT}), SHH (MB^{SHH}), group 3 (MB^{Grp3}) and group 4 (MB^{Grp4}) [6-12]. Interestingly, each group displayed distinct clinicopathological and biological characteristics and, most important, different outcomes. Therefore, in the updated WHO classification MB has been cathegorized according to molecular characteristics in addition to histopathological features [1].

1.4.1 WNT-activated MB

MB^{WNT} account for about 10% of cases and affect most frequently older children aged 6-10; a subset (~15%) of adult MB belongs to this subgroup. Tumors are located in the cerebellar midline/cerebellopontine angle and are almost exclusively characterized by a classic morphology. Notably, patients affected by MB^{WNT} display excellent outcomes, with an overall survival close to 100% [1]. The vast majority (approximately 90%) of MB^{WNT} carry mutant catenin β 1 (CTNNB1) protein, which drives constitutive WNT signaling activation. Hence, nuclear accumulation of β-catenin is a biomarker for WNT pathway activation. In addition, MB^{WNT} are characterized by chromosome 6 monosomy (~85% of cases) and mutated DEAD-box helicase 3 (DDX3X), TERT, SMARCA4 and tumor suppressor protein p53 (TP53).

1.4.2 SHH-activated MB

MB^{SHH} are extremely heterogeneous in terms of clinical, molecular and prognostic features. They account for approximately 30% of MB and arise more frequently in the cerebellar emispheric region. The consesus molecular classification has recognized two further subgroups based on TP53 mutational status, namely SHH-activated/TP53-mutant MB ($MB^{SHH/TP53m}$) and SHH-activated/TP53-wildtype MB ($MB^{SHH/TP53wt}$). $MB^{SHH/TP53m}$ are rare and occurr in young children aged 4-17 years. Unfortunately, metastatic spread is quite frequent at presentation and the prognosis of $MB^{SHH/TP53m}$ is dismal, with a 5-year overall survival of less than 40% [1]. Conversely, $MB^{SHH/TP53wt}$ are found in infants and young adults and carry better outcomes, with an estimated 5-year overall survival of 76% [1]. Morphological variants like desmoplastic/nodular and MB with extensive

nodularity can be considerent specific of the SHH-activated group, but cases of large cell/anaplastic MB are also seen, especially among $MB^{SHH/TP53m}$. From a molecular standpoint, SHH pathway activation in $MB^{SHH/TP53m}$ is associated with amplification of SHH, MYCN, GLI2, while mutations of PTCH1, SUFU and SMO drive the tumor initiation in $MB^{SHH/TP53wt}$. Recent evidence of an age-dependent biologic heterogeneity has emerged from methylation profiling data. In brief, PTCH mutations are uniformly distributed among infants, children and adults, whereas SUFU mutations are typical of the very young age (0-4); tumors arising in children harbour more frequently TP53 mutations and GLI2 amplifications; tumors arising in adults are characterized by SMO, DDX3X and TERT promoter mutations [13].

1.4.3 Non-WNT/non-SHH MB

Consensus MB^{Grp3} occurr in approximately 20% of patients and usually arise in very young children (0-4) with a higher incidence among males. This subgroup is notable for being clinically aggressive, with an overall survival rate of 50% to 60%. Thus indeed nearly half of patients present with metastases. Histologically, MB^{Grp3} display classic morphology, but a subset of cases show large cell/anaplastic morphology. MB^{Grp3} tipically carry MYC over-expression, which is associated to MYC amplification in a subset of cases (17%) [14]. Recurrent molecular alterations involve SMARCA4, OTX2, CTDNEP1, LRP1B, KMT2D, GFI1 and GFI1B. [1, 15].

Consensus MB^{Grp4} is the most common molecular subgroup (40%). Tumors belonging to this group affect more frequently children (>4 years) than adults and often display classic morphology. Prognosis is good among average-risk patients, while metastatic disease at the time of presentation is associated with poor outcomes [16]. MB^{Grp4} are characterized by recurrent alterations in KDM6A, SNCAIP and MYCN. Activation of the oncogene GFI has been observed in a subset of cases. Lmx1A, an homeobox transcription factor involved in the development of the normal cerebellum and midbrain, has been recently identified as an important transcription factor also in MB^{Grp4} [15, 17]. Isochromosome 17q is the most frequently detected chromosomal aberration, whereas chromosome 11 loss and chromosome 17 gain are recognized as negative prognostic factors [18].

The advent of molecular classification helped clinicians to identify patients with poor prognosis - particularly those with MB^{Grp3} and metastases - who could benefit of intensive therapy regimens, as well as those with favourable prognosis (e.g. MB^{WNT}) who could safely undergo minimized protocols in order to reduce treatment morbidity. However less toxic and subgroup- specific/targerted approaches are needed.

1.5 Integrating molecular subclassification into routine clinical practice

The translation of such important transcriptomic and methilomic findings into routinely applicable laboratory techniques carried practical issues [24]. A first attempt was done by Northcott and colleagues who proposed a panel of four antibodies (*DKK1, SFRP1, NPR and KCNA1)* to identify the subgroups [19]; unfortunately, this panel failed to prove reproducible among following studies. The same authors subsequently described an RNA-based Nanostring method which efficiently assigned cases to the corresponding molecular subgroups [20]. Further, Schwalbe and colleagues proposed a robust methylation profiling method based on DNA extraction from FFPE [21]. Despite being highly reliable and precise these methods were still too laborious and expensive to be incorporated into routine pathological evaluation of MB. Meanwhile, an immunohistochemical (IHC) panel of four antibodies (β-catenin, YAP1, GAB1 and filamin A) was developed to rapidly and faithfully identify MB^{WNT}, MB^{SHH} and $MB^{non\text{-}WNT/SHH}$ [22]. The diagnostic value of this panel was subsequently confirmed [23, 24] and applied on most laboratories on daily practice. Nonetheless, this panel still suffers from standardization difficulties across all centers and does not distinguish MB^{Grp3} from MB^{Grp4}. Thus indeed, further workup is often required to address this issue on a daily practice, such as FISH for MYC amplification [1]. However, one should be aware that despite being quite specific of Group3, MYC amplification is found mainly among infants, accounting for less than 25% of all MB^{Grp3}.

Medulloblastoma as a disorder of normal development

1.6 The importance of CGP migration in the development of MB

The normal development of the cerebellum is a complex pre and postnatal process in which specific extracellular molecules, like mitogens and cytokines, regulate survival, proliferation, migration and differentiation of neural stem cells [25]. Hedgehog-induced medulloblastoma (MB) has been shown to derive from cells related to cerebellar granule neuron precursors (CGP) [26]. In the developing cerebellum, CGP proliferate and migrate from the external granule layer to the

adjacent inner external granule layer. Finally, they reach the internal germinal layer upon concentration-dependent signalling promoted by Shh, a highly conserved mitogenic glycoprotein secreted by Purkinje cells. Once arrived at their permanent location, the internal germinal layer, GCP exit from the cell-cycle and differentiate. Since sustained proliferation increases the risk of tumorigenesis, the migration of CGP, which acts as an indirect regulator of cell proliferation, has been investigated in relation to MB development.

In a double knock-out (Ptch1+/−/Tis21−/−) mouse model, the downregulation of the chemokine Cxcl3 resulted into a significant increase of MB by preventing GCP to migrate towards the internal germinal layer and keeping them in the proliferative niche of the external granular layer [27]. Despite different mechanisms, Haag and colleagues illustrated a mouse model with similar phenotype: in their Ptch1(+/-) Nos2(-/-) mice the deficiency of Nos2, an inducible nitric oxide synthase, promoted the occurrence of MB through retention of proliferating GCPs in the external granular layer and impaired migration upon Gap43 knock-down [28]. Interestingly, a follow-up study demonstrated that sustained administration of the chemochine Cxcl3 in the cerebellum of Ptch1+/−/Tis21−/− mice affected with MB led to complete regression of the lesions. These results indicate that the induction of GCP migration, resulting into further differentiation, may open new treatment perspectives, at least at early stages of disease [29].

1.7 The JAM protein family

Junctional adhesion molecule (JAM)-A, -B, -C are cell-cell adhesion molecules of the immunoglobulin superfamily which display a wide tissue distribution, both during development and in the adult organism [30] (Tab.1).

Table 1. JAM-A, -B, -C: corresponding genes and expression patterns (adapted from Ebnet et. al [30])

Jam family member	Gene name	Tissue distribution
JAM-A (h: F11R, JAM-1) (m: F11R, JAM-1)	h: F11R, JAM1 m: F11r, Jam1	EpC, EC, Sertoli cells,leukocytes,platelets, HSC,NG2 glia cells
JAM-B (h: JAM-2, VE-JAM) (m: JAM-3)	h: JAM2, VEJAM m: Jam2, Vejam	EC, Sertoli cells,HSC, BM stromal cells, retinal ganglion cells, myoblasts
JAM-C (h: JAM-3) (m: JAM-2)	h: JAM3 m: Jam3	EpC, EC, leukocytes(h), platelets (h), male germ cells,HSC, Schwann cells, neurons, neural stem cells, myocytes, Müller glia cells, vascular SMC

As long as we know, they are involved in multiple cellular processes including cell-cell adhesion, shape, polarity, motility, migration and mitotic spindle orientation. Based on these properties they take part to the formation and manteinance of epithelial and endothelial barriers, hemostasis, angiogenesis, hematopoiesis and the early development of several tissues including germ cells, central and peripheral nervous system.

1.7.1 Structural features

The JAM proteins, belonging to the CTX ("cortical thymocyte marker in Xenopus") subfamily of the immunoglobulin superfamily, are characterized by a cytoplasmic tail, a single trasmembrane domain and two IgSF domains, a membrane-distal V-type and a membrane-proximal C2-type Ig domain.

The biologic function of JAM molecules is associated with two highly conserved structural motifs. The first is a tripeptide in the D1 Ig domain which mediates, in JAM-A, the homodimerization in cis; this motif is also conserved in JAM-B and JAM-C. Cis-dimerization also requires additional residues described in the D1 domain of JAM-A that are not found in the crystal structure of JAM-B and JAM-C, thus suggesting that the forces between monomers might change among the three JAMs with functional implications. Cis-dimerization is an early event, which happens during the secretory pathway. Once reached the cell membrane, multi trans-homophilic interactions among cis-dimers of opposing cells are established, resulting into cell-cell contact at cell junctions [31]. However, the primary function of such interactions does not correspond to strengthening cell-cell adhesion since trans-homophilic JAM-JAM bridges seem rather weak. JAM -A, -B and –C can also interact with other membrane proteins both in cis and trans. JAM-JAM trans interactions may happen among between different cell types giving rise to a variety of biological processes.

The second highly conserved structural region is a PDZ domain-binding motif at the COOH terminus which is always involved in protein-protein interactions between JAMs and their direct binding partners. Interestingly, most scaffolding proteins interacting with JAMs harbour multiple protein-protein interaction domains, which serve to assemble or recruit signalling complexes at specific sites of cell-cell contacts such as the tight junctions (TJ) [32]. Since each monomer within a JAM dimer independently interacts with different proteins, cis-dimerization mediates the

crosslinking between cytoplasmic signaling proteins. JAM proteins can also exist in complex with other protein and play a regulatory role independent of cell-cell contact: for instance, the JAM-associated protein can be laterally recruited into a protein complex to modify integrin-mediated signaling [33].

1.7.2 The role of JAMs in the development of the cerebellum

JAM-A,-B,-C are expressed by cells of central nervous system (CNS) during both developmental phases and in the adult life. JAM-A has been found to play a role in the development of the forebrain as a regulator of mitotic spindle orientation in radial glia cells of the ventricular and subventricular zones [30]; mouse model data also indicated that JAM-A is a marker of NG2-glia [34]. On the other hand, JAM-B and JAM-C are critical for the development of the cerebellum. As previously mentioned, during postnatal development the cerebellar granule neurons (CGN) proliferate in the external granule layer (EGL), become postmitotic, polarize, extend a radial process and finally migrate through the molecular layer in order to populate the internal granule layer (IGL), where they differentiate towards more mature neurons. The inward migration of CGN precursors is allowed by the presence of the radial fibers of Bergmann's glial cells, which are used as a guide towards the IGL from CGN precursors (Fig. 1). The interaction between Bergmann's glia fibers and CGN is mediated by trans-homophilic/heterophilic bounds between JAM-B and JAM-C, with CGN expressing JAM-C and Bergmann's glial cells expressing both JAM-B and JAM-C.

Figure 1. JAM-B and JAM-C regulate migration of CGN during CNS development (adapted from Ebnet et al. [30]).

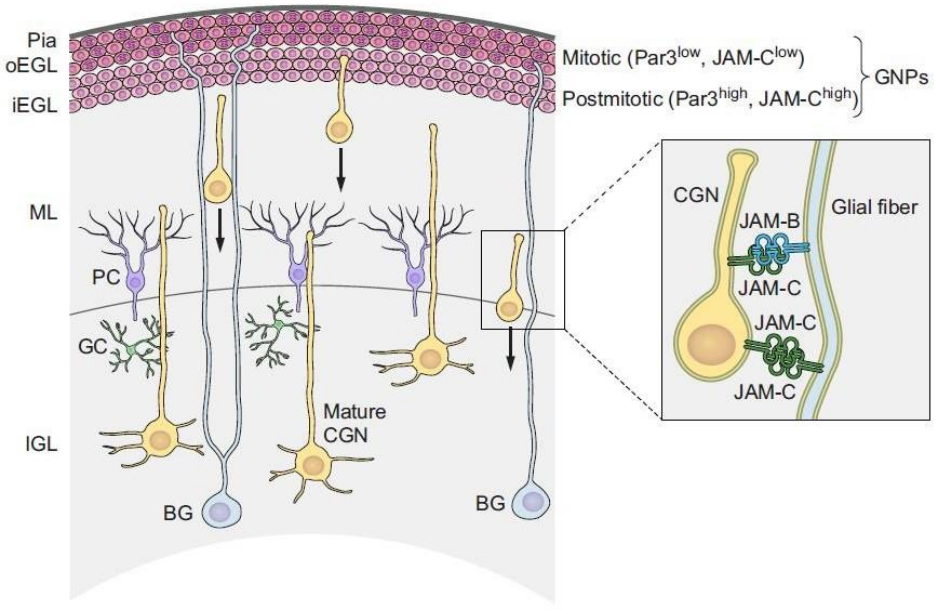

The expression of JAM-C at cell surface is regulated by PAR-3, while PAR-3 expression is downregulated by PAR-3 ubiquitine ligase Siah [35]. Interestingly, as long as the CGN stay in the outern EGL, Siah is active, PAR-3 levels are low and JAM-C is not expressed. Once arrived in the inner layer of the EGL, upregulation of PAR-3 and surface localization of JAM-3 enable CGN progenitors to interact with Bergmann's glia fibers and to use them as a guide in their path towards the IGL.

1.7.3 The role of JAMs in tumorigenesis

The role of all JAM proteins in tumor development has not been studied in detail, but to date JAM-A has been investigated more extensively than JAM-B and JAM-C. Nontheless, since both hyper-expression and reduced expression of JAM-A have been associated with poor outcomes, its functions in cancer remains unclear. Indeed, high expression of JAM-A has been correlated with dismal prognosis in hematopoietic tumors such as multiple myeloma and diffuse large B-cell lymphoma (DLBCL) and in several epithelial neoplasms like lung and nasopharingeal carcinomas [36, 37, 38, 39]. However, low expression of JAM-A has been associated with worst outcomes in renal, pancreatic and gastric cancer [40, 41, 42]. Conflicting data have emerged also in breast cancer, as both high and low expression of JAM-A have been associated with poor prognosis [43, 44].

Flow citometry performed in triple-negative breast cancer cell cultures demonstrated that JAM-A was overexpressed in a population of cancer cells with features close to tumorigenic cancer stem cells and independently induced self-renewal [45]. Further evidence of JAM-A being associated with stemness was provided by Rosager et Al, who found that JAM-A expression was higher in glioblastoma than in WHO grade II and III gliomas and co-localized with a well-known stem cell marker, CD133 [46]. These data were supported by Xu et Al., who demonstrated that high expression of JAM-A sustained stemness in DLBCL by inducing higher expression of CD133 both in cell lines and in vivo; it also correlated with cell invasion and epithelial-to-mesenchymal transition. Interestingly, the administration of Lenalidomide led to reduced tumor aggressiveness in a murine xenograft model harbouring JAM-A-overexpressing DLBCL cells by promoting degradation of JAM-A mRNA [37].

The role of CD133 as a marker of cancer stem cells (CSC) that sustain tumor growth has been widely investigated in MB. In a retrospective study CD133 hyper-expression was associated with increased metastic spread and poor outcome in MB^{Grp3} [47]. Further support to these findings

came from in vitro studies, which demonstrated a strong enrichment of CD133 in MB^{Grp3} cell cultures; functional data showed that $CD133^{+}$ cell populations resulted into larger and more aggressive tumors when xenografted in mice compared to $CD133^{-}$. According to the proposed cellular mechanism, a CD133-dependent activation of the signal transducers and activators of transcription-3 (STAT3) pathway seems to drive tumorigenesis in MB^{Grp3} through regulation of c-MYC [48]. Since inhibition of CD133-dependent STAT3 activation could represent a potential therapeutic strategy for MB^{Grp3}, the putative biological relation between JAM-A and CD133 needs to be investigated in MB.

Despite being less studied than JAM-A, JAM-C hyperexpression has been associated with increased biological aggressiveness and poor outcome in a variety of tumors, including acute myeloid leukemia, gliomas, melanoma and lung cancer [49-52]. JAM-C may be implicated directly in increased aggressiveness by promoting cancer cell migration and metastatic spread, while JAM-B seems involved in the dimerization of JAM-C, thus influencing tumor aggressiveness indirectly [53].

2. Aims

The aim of this study was to to examine gene and protein expression of JAM molecules in pediatric MB, by relying on open access large datasets and a clinical sample.

3. Methods

Gene expression analysis

3.1 Gene expression datasets

Two publically available datasets stored in the R2: Genomic Analysis and Visualization Platform (http://r2.amc.nl) were used for the gene expression analysis. The first dataset [Cancer Cell. 2017 Jun 12;31(6):737-754.e6. doi: 10.1016/j.ccell.2017.05.005. Intertumoral Heterogeneity within Medulloblastoma Subgroups] contains the gene expression profile of 763 fresh frozen primary medulloblastoma samples measured by the Affymetrix Human Gene 1.1 ST Array (GEO ID: GSE85217). The second data set [R2 internal identifier: ps_avgpres_mb500affym223_u133p2; Medulloblastoma Landmark Study, Pfister – 223- MAS5.0 – u133p2] contains the gene expression profile of 223 tumors measured by the Affymetrix Human Genome U133 Plus 2.0 platform (GEO ID: GSEXXX). Patients older than 18 years at diagnosis were excluded from the analysis.

3.2 Statystical analysis

Log2-transformed gene expression values were utilized for the analyses. Gene symbol was the reference annotation. When multiple probe sets were present in the gene expression platform for one gene, the expression of the probe set with the highest expression was associated to the gene using the R2: Genomic Analysis and Visualization Platform (http://r2.amc.nl).

The significance of the difference between mean expression values was determined by one-way ANOVA test when the comparison involved more than two groups. Post-hoc analysis was assessed by Tukey's multiple comparisons test. Prism 6.1 (GraphPad Software, Inc.) was used to perform statistical analyses.

Experimental study

3.3 Case selection

All cases of MB operated over a period of 21 years (1996-2017) in the Neurosurgery Unit of Giannina Gaslini Institute of Genoa were retrieved. Inclusion criteria for the study cohort consisted of:

1. Age lower than 18 years.

2. Availability of the main clinico-demographic data.

3. Presence of adequate tumor tissue in FFPE blocks.

4. Confirmation of the histological diagnosis of MB according to the most recent WHO Classification of CNS tumors [1].

3.4 Histopathology

Hematoxylin and eosin (H&E) stained slides of all cases were reviewed by one surgical pathologist (CB) and one pathologist with experience in Neuropathology (PLP). Reticulin preparations were obtained for each case in order to evaluate desmoplasia. Cases were histologically subclassified as classic MB (C-MB), desmoplastic/nodular MB (D/N-MB), MB with extensive nodularity (MBEN), large cell (LC-MB) and anaplastic MB (A-MB). Large cell and anaplastic MB were combined and diagnosed as large cell/anaplastic MB (LC/A-MB) according to the current WHO Classification of the CNS [1]. The presence of additional morphological features (neurocytic/ganglionic differentiation, astrocytic differentiation, focal large cell morphology, focal anaplastic morphology e.g.) or rare morphological variants (melanotic MB, myogenic MB e.g.) was also recorded.

Representative blocks were chosen to perform immunohistochemical analyses. When available, specimen containing normal cerebellar tissue were also submitted to IHC in order to obtain an internal control for selected antibodies (JAM-B, JAM-C).

Clinical data as well as follow-up information were available in a subset of cases from a previous study [47].

3.5 Immunohistochemistry

Immunohistochemical reactions were performed at Giannina Gaslini Institute (Genoa) and Spedali Civili (Brescia, courtesy of Prof. P.L. Poliani) as follows. Two µm sections were cut from paraffin embedded cells blocks. In brief, sections were de-waxed, re- hydratated and endogenous peroxidase activity blocked with 0.3% H_2O_2 in methanol for 15 minutes. Epitope retrieval was obtained by microwave or a thermostatic bath in 1.0 mM EDTA buffer pH 8.0. Sections were then washed, pre-incubated in blocking buffer containing 5% normal goat serum in Tris-HCl for 5 minutes and incubated for 60 minutes (β-catenin, YAP1, GAB1, FilaminA) or overnight (F11R/JAM1, JAM2, JAM3) with primary antibody in Tris/1% Bovine Serum Albumin (BSA). The following primary antibodies have been used: mouse monoclonal anti-β- catenin (1:1000, 15B8, Sigma-Aldrich), mouse monoclonal anti-YAP1 (1:50, sc101199, Santa Cruz), rabbit monoclonal anti-GAB1 (1:50, ab113486, Abcam), mouse monoclonal anti-FilaminA (1:50, 10R-F113a, Fitzgerald), rabbit polyclonal anti-F11R (1:50, Sigma-Aldrich), mouse monoclonal anti- JAM2 (1:30, 1G4, Sigma-Aldrich), rabbit polyclonal anti-JAM3 (1:30, Sigma-Aldrich). Sections were then washed in Tris-HCl buffer prior to incubation for 30 minutes with the secondary antibody (ChemMATE Envision Rabbit/Mouse, DAKO). Signal has been revealed with diaminobenzydine (DAB) and slides counterstained with Hematoxylin.

Specific positive and negative controls were selected for assessing anti-F11R, JAM2 and JAM3 reactivity.

Samples were examined unaware of the clinical data. The staining evaluation of β-catenin, YAP1, GAB1 and FilaminA was conducted according to Ellison [22]. JAM-A, -B, -C expression was scored semi-quantitatively as staining intensity (0=no visible staining; 1=weak; 2=moderate; 3=strong).

3.6 Nanostring N-counter assay

Molecular classification was available in a subset of cases included in a previous study [54]. Subgroup affiliation was determined at the Hospital for Sick Children (Toronto, ON, Canada) applying the NanoString nCounter Elements™ assay. All procedures were performed following the manufacturer's instructions as follows (NanoString Technologies, Seattle, WA, USA).

Total RNA (100 ng) was extracted using using RNeasy kits (Qiagen). RNA concentration and integrity were assessed with NanoDrop (Thermo Fisher Scientific, Waltham, MA, USA) and Bioanalyzer (Agilent Technologies, Inc., Santa Clara, CA, USA), respectively.

For group assignement, a 22-genes CodeSet was applied, including specific gene-signatures for each subgroup as originally described by Northcott [20]: WNT (WIF1, TNC, GAD1, DKK2, EMX2), SHH (PDLIM3, EYA1, HHIP, ATOH1, SFRP1), Group C (IMPG2, GABRA5, EGFL11, NRL, MAB21L2, NPR3), Group D (KCNA1, EOMES, KHDRBS2, RBM24, UNC5D, OAS1). In addition, three housekeeping genes (ACTB, GAPDH, and LDHA) were included in the CodeSet to normalize the biological data.

The probes developed by IDT Technologies were diluted in probe pools and subsequently hybridized with 100-300 ng RNA, along with hybridization buffer and TagSet reagents. Following incubation (21h) at 67°C, the samples were trasferred to the nCounter® PrepStation (NanoString) to undergo purification steps and cartridge preparation. The resulting cartridges were loaded to nCounter® Digital Analyzer (NanoString), a multi-channel epifluorescence scanner which provided all gene counts. Clustering analyses of the samples were subsequently performed.

3.7 Statystical analysis

We explored the association between JAM expression and clinical characteristics by employing first univariate analyses, namely Pearson correlation, T-test and chi-square. Subsequently, multivariate regression were conducted adjusting by relevant confounders. In order to examine whether JAM would reliably differentiate between different histological subtypes, we used ROC curve analysis; cutoff value with the best trade off of sensitivity and specificity are reported. Finally, survival was examined first using Kaplan Meyer analyses followed by Cox regression to examine the impact of continuous or categorical predictors.

4. Results

Gene expression analysis

4.1 Clinicopathological features

We assessed the expression of F11R, JAM-2 and JAM-3 genes in two independent medulloblastoma gene expression datasets (Table 1). As previously stated, patients older than 18 were filtered out from these data sets (125 and 39 patients for Cavalli and Pfister, respectively). The main demographic and clinico-pathological features of both cohorts are summarized in Tab. 2.

Table 2. Demographic and clinicopathological characteristics of MB patients included in the gene expression analysis.

Variables	Cavalli (n)	Pfister (n)
Cases	638	223
Age		
Age <4 years	173	48
Age 5-18 years	465	136
Gender		
Male	414	
Female	214	65
na	10	118
K	0	1
Pathology		
C	346	-
D/N	88	-
EN	17	-
LC/A	66	-
na	121	-
Molecular subgroup		
MB^{WNT}	52	13
MB^{SHH}	151	31
MB^{Grp3}	131	55
MB^{Grp4}	304	85
Metastasis at diagnosis		
Absence	339	-
Presence	167	-
na	132	-
Outcome		
A	403	-
D	151	-
na	84	-

4.2 Expression of F11R, JAM-2 and JAM-3 among the consensus molecular subgroups

4.2.1 F11R, JAM-2 and JAM-3 are differentially expressed among MB subgroups

One-way ANOVA test assessed the presence of any significant difference among the four subgroups on the remaining 638 and 184 patients. Analysis evidenced that among the four subgroups a significant differential expression of F11R, JAM-2 and JAM-3 existed in both datasets (ANOVA p value<0.0001, Fig. 2).

Figure 2. ANOVA analysis of F11R, JAM2 and JAM3 expression among medulloblastoma patient subgroups.

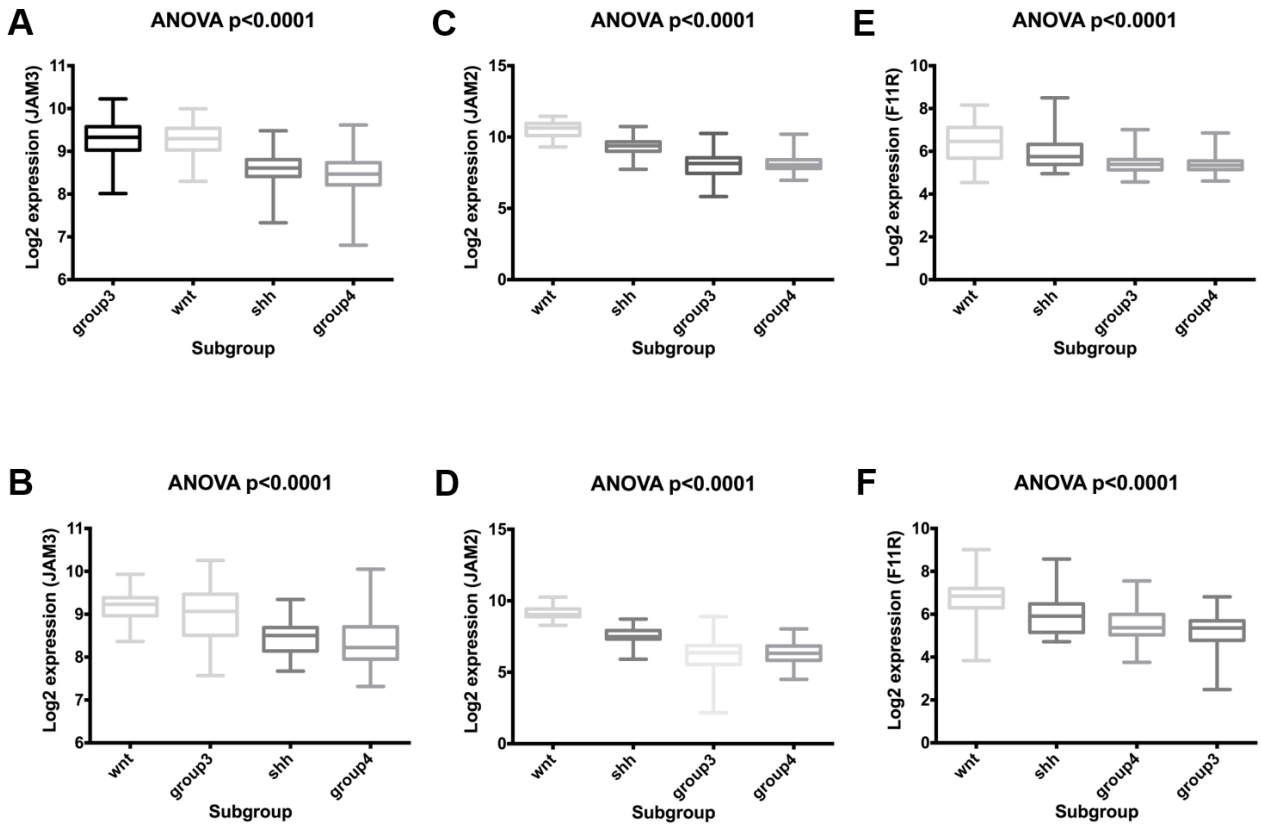

The box and whisker plots show the expression of F11R (E and F), JAM2 (C and D) and JAM3 (A and B) in two independent medulloblastoma gene expression data sets (A, C, E: Cavalli; B, D, F: Pfister). The box and whisker are sorted by decreasing order of median expression value. Plots are entitled with the one-way ANOVA p value. We considered significant a p value<0.05.

4.2.2 JAM-3 is differentially expressed between MB^{Grp3} and MB^{Grp4}

Post-hoc analysis provides a statistical method to identify significant differences among the groups analyzed in an ANOVA test. Post-hoc analysis of F11R, JAM-2 and JAM-3 in the two independent data sets (Fig. 3) showed that:

- F11R expression was significantly different between the following couples of subgroups in both datasets: MB^{WNT} and MB^{Grp4}; MB^{WNT} and MB^{Grp3}; MB^{SHH} and MB^{Grp3}; MB^{SHH} and $MB^{Grp4.}$

- JAM-2 expression was significantly different between the following couples of subgroups in both datasets: MB^{WNT} and MB^{Grp4}; MB^{WNT} and MB^{Grp3}; MB^{SHH} and MB^{Grp3}; MB^{SHH} and $MB^{Grp4.}$; MB^{WNT} and MB^{SHH}.

- JAM-3 expression was significantly different between the following couples of subgroups in both datasets: MB^{WNT} and MB^{Grp4}; MB^{SHH} and $MB^{Grp3.}$; MB^{WNT} and MB^{SHH}. Interestingly, we observed a strong differential expression (p<00001) of JAM-3 between MB^{Grp3} and MB^{Grp4}.

Figure 3 –Post hoc analysis of F11R, JAM-2 and JAM-3 expression among medulloblastoma patient subgroups.

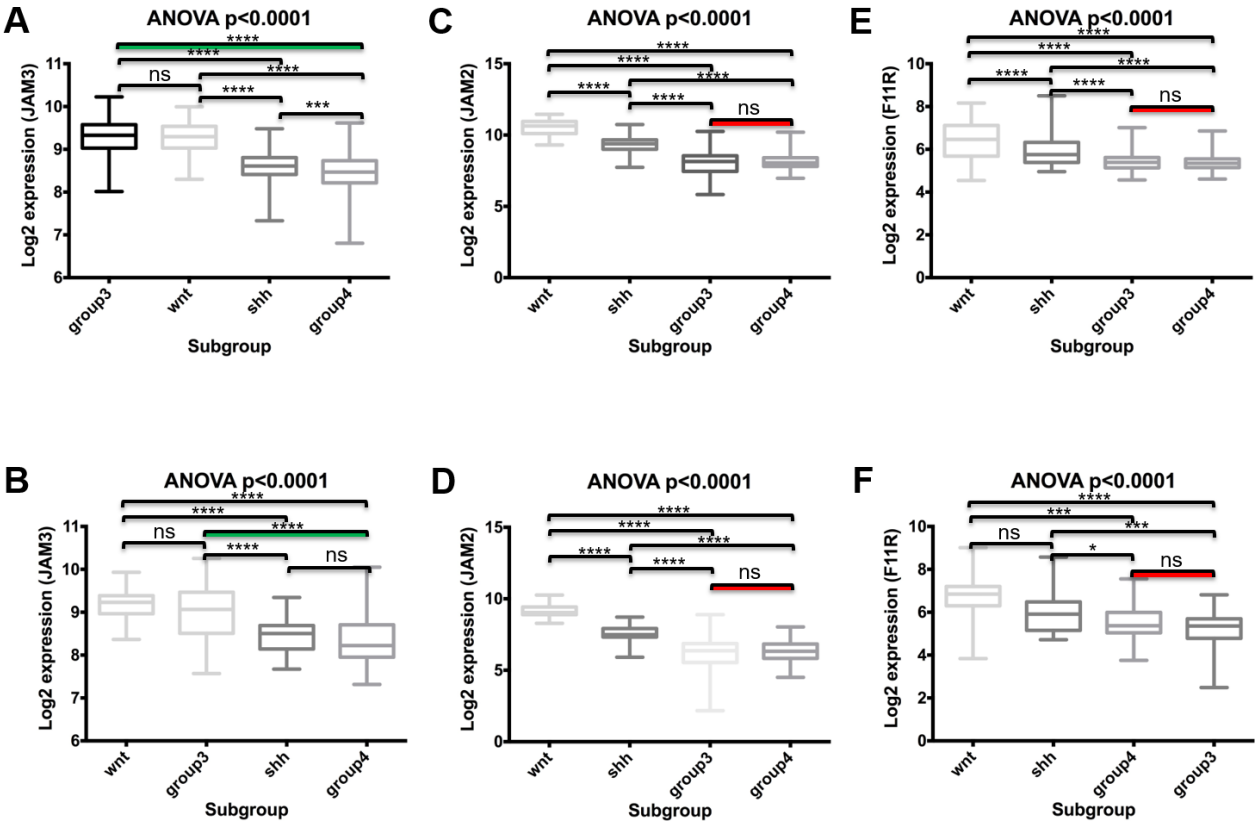

Compared to F11R and JAM2 which do not show any significant difference (red bars), JAM3 is differentially expressed (green bars) between MB^{Grp3} and MB^{Grp4} in both datasets (A, Cavalli; B, Pfister). For each comparison, Tukey's adjusted p value is reported on the black bar. * stands for p <0.01. *** stands for p<0.0001. **** stands for p<0.00001. ns stands for not significant. We considered significant a p value<0.05.

JAM-3 expression did reliably discriminate between MB^{Grp3} and MB^{Grp4} on the basis of a ROC curve analysis (AUC=0.93, SE=0.013, 95%CI: 0.90 – 0.96, p<0.001). For instance, a cutoff value in JAM-3 expression of 8.879 yielded a sensibility of 84.0% and a specificity of 84.5% (Fig. 4).

Figure 4. Discrimination of subgroups using JAM-3 expression: ROC curve analysis

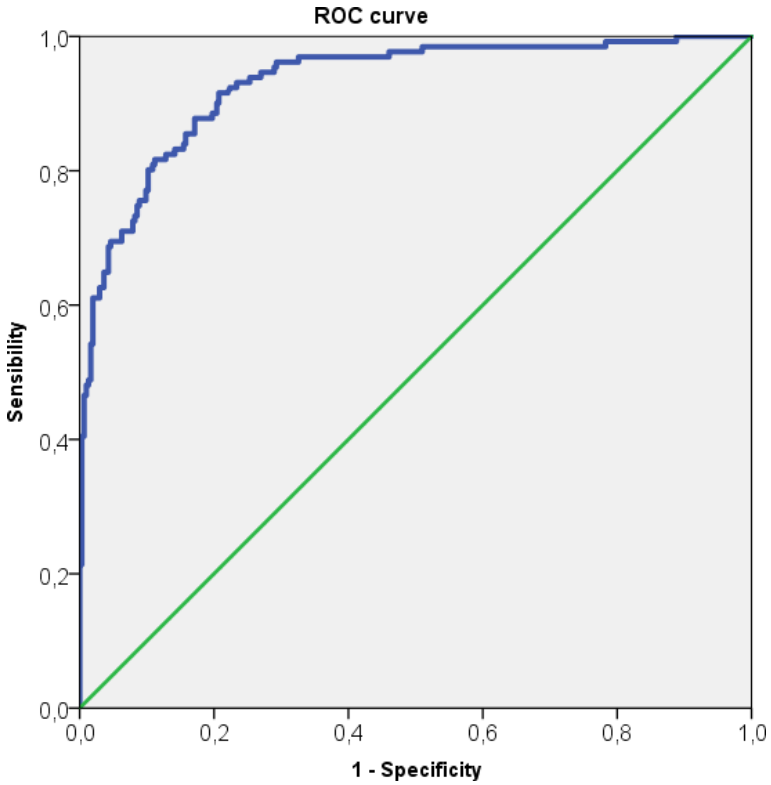

4.3 Associations between JAM-3 and clinicopathological characteristics

4.3.1 JAM-3 expression is significantly higher among LC/A

Table 3. Associations between JAM-3 expression (quintile split) and demographic/clinicopathological features

		% with high expression	*p*
Age	≤36m	11.8	0.735
	>36m	12.9	
Gender	F	11.1	0.065
	M	16.4	
Pathology	C	12.7	0.007
	D/N	3.4	
	LCA	19.4	
	MBEN	0.0	
Metastasis	Yes	10.6	0.050
	No	16.8	

JAM-3 expression correlated slightly with age (R=0.11, p=0.006) (Fig. 5).

Figure 5. Correlation between JAM-3 expression and age

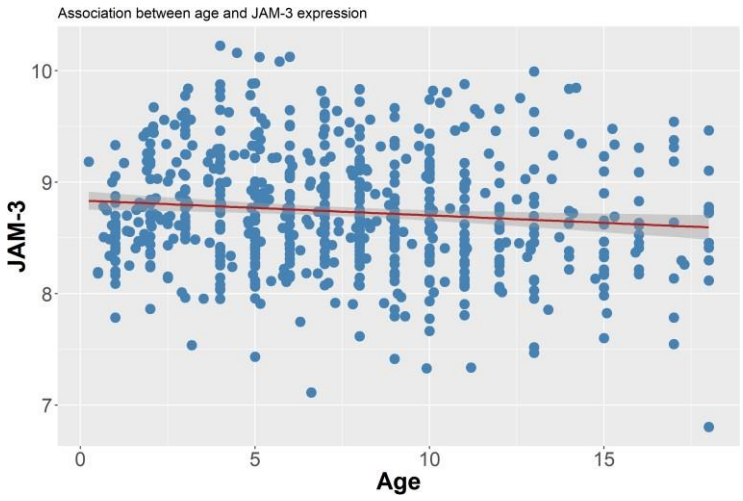

Post-hoc analysis revealed that JAM-3 expression was significantly higher among LC/A than among other variants (Fig. 6).

Figure 6. JAM-3 expression by pathology

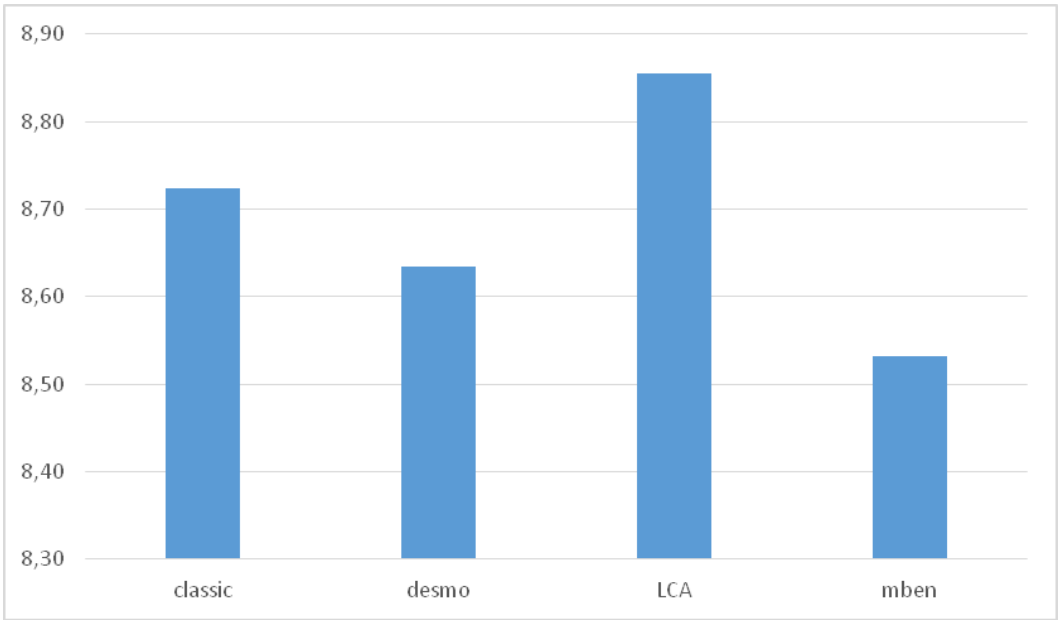

4.4 Prognostic value of JAM-3 in MB

4.4.1 High expression of JAM-3 is associated with shorter survival

Mean survival was 14.1 (95%CI 12.7 – 15.4) years. Among subjects with the highest quintile of JAM-3 expression, mean survival was significantly shorter than among the remainder of the sample (high JAM-3: 9.00; 95%CI: 7.21 – 10.79; low JAM-3: 14.42; 95%CI: 12.92 – 15.93, Logrank chi squared=9.24, p=0.002) (Fig. 7). This translates to an Hazard Ratio (HR) of 1.86 (95%CI: 1.24 – 2.80) in Cox regression for the quintile split, and to a increased likelyhood of 36% for each point change in continuous JAM-3 expression (beta=0.31, HR=1.36, 95%CI: 1.01 – 1.84, p=0.043).

Figure 7. Survival by JAM-3 expression

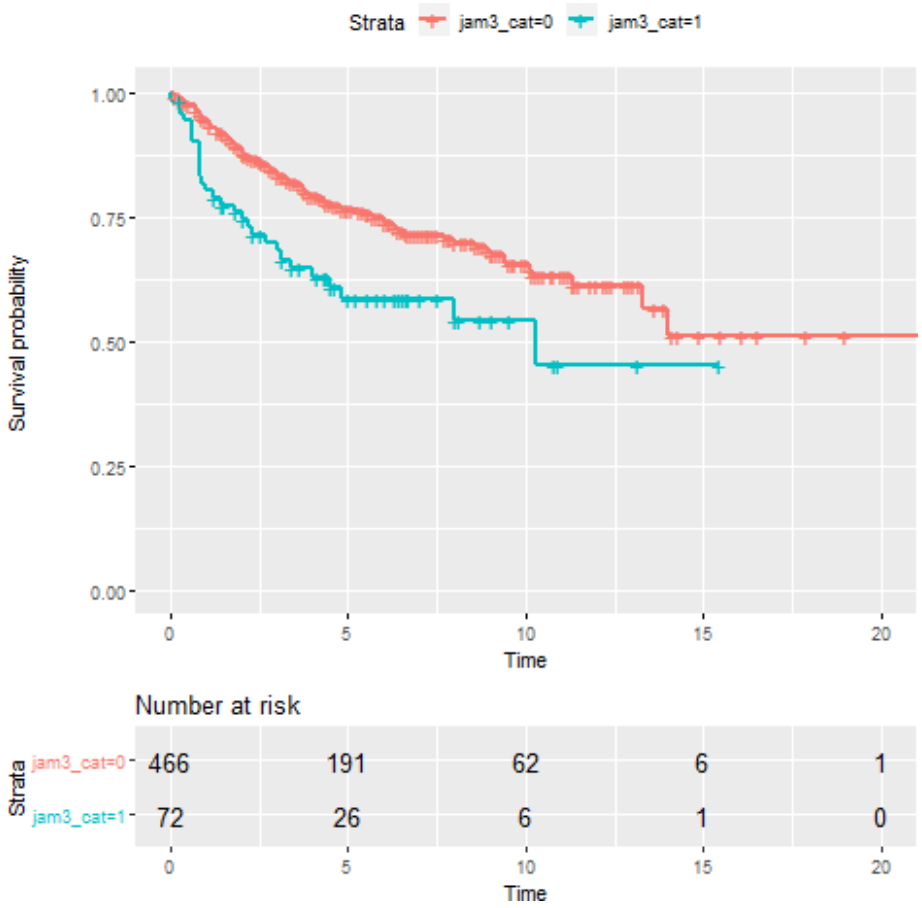

4.4.2 Multivariate analysis/ JAM-3 expression

With the following analyses we sought to examine whether the association between JAM-3 expression and survival was still significant after accounting for covariates (age, gender) and whether it outperformed pathology and molecular subgroup.

Either using a quintile cutoff or a continuous measure of JAM-3 expression, adjusting for age and gender did not change the results signficantly. With the quintile-split approach, in a Cox regression JAM-3 had a Hazard Ratio (HR) of 1.91 (95%CI: 1.27 – 2.87, p=0.002) for a shorter survival. Using the continuous value of JAM-3 expression, each point change corresponded to a 36% increased likelyhood of shorter survival (beta=0.33, HR=1.39, 95%CI: 1.02 – 1.90, p=0.035).

In the univariate model, LC/A pathology was associated with a significantly lower survival compared with Classic MB (Model chi square 17.1, gl=3, p=0.001; HR=2.47; 95%CI 1.58 – 3.87, p<0.001).

Table 4. Cox-Regression model: pathology predicting survival

	B	SE	Wald	gl	Sign.	Exp(B)	95,0% CI per Exp(B)	
							Lower	Upper
Classic (ref)	-	-	19,832	3	,000	-	-	-
Desmo	-,297	,311	,916	1	,338	,743	,404	1,365
LCA	**,907**	**,228**	**15,776**	**1**	**,000**	**2,478**	**1,583**	**3,877**
MBEN	-,556	,717	,602	1	,438	,573	,141	2,337

JAM-3 expression was no longer significant after adjusting for pathology (JAM-3 as continuous: HR=1.20; 95%CI: 0.87 – 1.65, p=0.28; categorical: HR=0.60, 95%CI: 0.15 – 2.45, p=0.48). In the univariate model, WNT was associated with a significantly longer survival compared with the SHH group, while Group 3 had a significantly lower survival (Model chi square 26.2, gl=3, p<0.001).

Table 5. Cox-Regression model: subgroups predicting survival

	B	SE	Wald	gl	Sign.	Exp(B)	95,0% CI per Exp(B)	
							Inferiore	Superiore
SHH (ref)			20,491	3	,000			
WNT	-1,540	,607	6,441	1	,011	,214	,065	,704
Group 3	,633	,240	6,946	1	,008	1,882	1,176	3,013
Group 4	,018	,223	,007	1	,934	1,018	,658	1,576

Again, JAM-3 expression was no longer significant after adjusting for molecular subgroup, if JAM-3 was entered as continuous (HR=1.37; 95%CI: 0.91 – 2.04, p=0.13) but retained a significant association with survival if was entered as a categorical variable (HR=1.96, 95%CI: 1.14 – 3.38, p=0.016). Also, Group 3 was no longer significantly associated with survival after adjusting for JAM-3 (HR=1.36, 95%CI: 0.78 – 2.38, p=0.28).

4.5 Clinicopathological features

A total of 65 cases were selected according to inclusion criteria. Fifteen (of 80) cases were excluded: 1 case of a MB arisen in a young adult; 12 cases with both blocks and slides unavailable for review and further characterization; 2 cases felt not to fulfill the diagnostic criteria for MB.

The resulting case series (n=65) corresponded to 63 patients, since both primary tumor and relapse were enlisted for 2 patients. Patients included 22 females and 41 males, with median age at diagnosis of 6,19 years (range 11 months-14 years). Of these, 17 patients were ≤36 months-old (infants) and 46 were >36 months-old.

Tumors arose predominantly in the vermis (89%), with a minority of cases involving the emispheres (8%) or both vermis and emispheres (3%). Imaging data also indicated that 38% of patients presented metastasis at diagnosis.

Gross total resection (GTR) was achieved in 71% of cases, subtotal resection in 29%.

Histologic classification showed that 63% (n=41/65) of cases were classic MB, 13% (n=8/65) D/N MB, 3% (n=2/65) ENMB and 21% (n=14/65) LC/A MB.

Cases were staged according to current consensus protocols and treated at Giannina Gaslini Institute (Neuro Oncology Center, D.ssa M.L. Garrè). Eleven patients presented with metastases (n=11/29, 38%).Twelve patients relapsed (n=12/29, 41%) and twelve patients died (n=12/40, 30%). The average follow-up was 47,32 months (range 9,18-130,10).

4.6 Molecular subgrouping

4.6.1 Immunohistochemistry accurately defines consensus MB^{WNT}, MB^{SHH} and MB$^{nonWNT/SHH}$.

The following table reports the correspondence between immunohistochemistry and Nanostring on molecular subgroup assessment. Only two cases showed conficting results (in bold, Tab. 6). One case, categorized as MB^{WNT} from Nanostring, displayed immunohistochemical features more consistent with MB$^{nonWNT/nonSHH}$: negative to focally cytoplasmic β-catenin, negative YAP1/GAB1/Filamin A. The second case, which belonged to Group4 according to Nanostring, exhibited focal myogenic differentiation and displayed contrasting immunohistochemical results (nuclear β-catenin in a subset of cells ->10%-, positive YAP1, negative GAB1, positive Filamin A). For statistical purposes, we decided to categorize these cases according to Nanostring. In fact, in the first case immunohistochemistry was considered unreliable because of pre-analytical issues (poorly preserved tissue). In the second case, Nanostring classification was adopted because of the known tendency of MB with myogenic differentiation (even focal) not to align on immunohistochemistry with genetically defined subgroups [Gupta].

Table 6. Concordance between immunohistochemical and Nanostring subgrouping

			SUBGROUP BY IHC			Totale
			WNT	SHH	***NON***	
SUBGROUP BY NANOSTRING	WNT	N	1	0	***1***	2
		% in SUBGR_NANOSTR	50,0%	0,0%	***50,0%***	100,0%
		% in SUBGR_IHC	50,0%	0,0%	***3,8%***	5,6%
		% del totale	2,8%	0,0%	***2,8%***	5,6%
	SHH	N	0	8	0	8
		% in SUBGR_NANOSTR	0,0%	100,0%	0,0%	100,0%
		% in SUBGR_IHC	0,0%	100,0%	0,0%	22,2%
		% del totale	0,0%	22,2%	0,0%	22,2%
	GROUP3	N	0	0	10	10
		% in SUBGR_NANOSTR	0,0%	0,0%	100,0%	100,0%
		% in SUBGR_IHC	0,0%	0,0%	38,5%	27,8%
		% del totale	0,0%	0,0%	27,8%	27,8%
	GROUP4	N	***1***	0	15	16
		% in SUBGR_NANOSTR	***6,3%***	0,0%	93,8%	100,0%
		% in SUBGR_IHC	***50,0%***	0,0%	57,7%	44,4%
		% del totale	***2,8%***	0,0%	41,7%	44,4%
Total		n	2	8	26	36
		% in SUBGR_NANOSTR	5,6%	22,2%	72,2%	100,0%
		% in SUBGR_IHC	100,0%	100,0%	100,0%	100,0%
		% del totale	5,6%	22,2%	72,2%	100,0%

4.7 Immunohistochemical expression of JAM-A, JAM-B and JAM-C in MB

JAM-A was negative among all tested cases (n=47), with positive internal controls (endothelial cells).

JAM-B was tested in 8 cases (Fig. 8). Staining pattern was cytoplasmic and paranuclear (Golgi pattern) in cases scored 1+ and 2+; interestingly, one case scored 3+ demonstrated also nuclear staining. Five cases had weak (1+) expression (62.5%) and were distributed as follows based on molecular classification and pathology: 1 MB^{SHH} (LC/A), 2 MB^{Grp3} (both of them classic MB) and 2 MB^{Grp4} (1 LC/A, 1 classic). One SHH-activated MB with D/N morphology had moderate (2+) expression (12.5%) . Two WNT-activated MBs with classic morphology displayed strong expression (3+) (25%).

Figure 8. Immunohistochemical expression of JAM-B

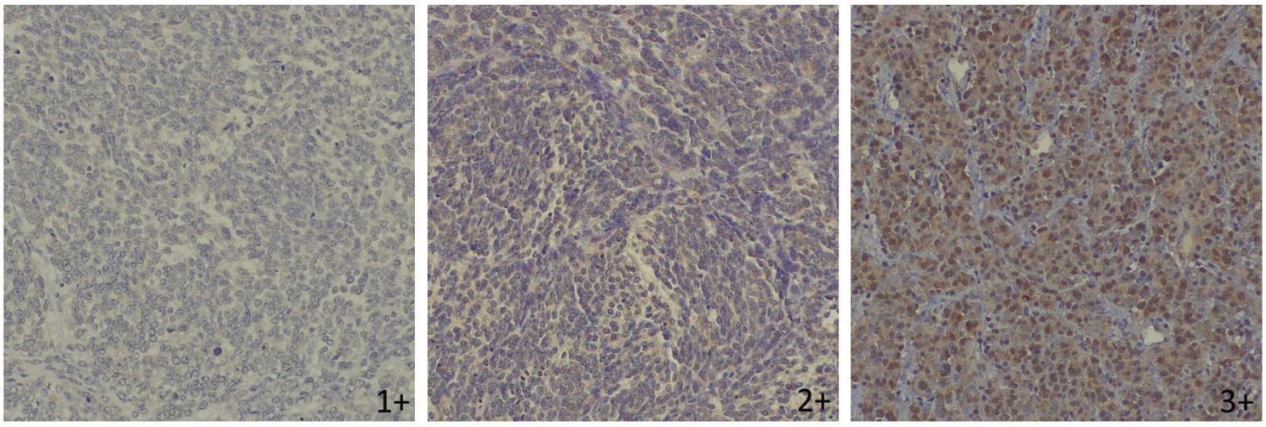

JAM-C was tested in 27 cases (Fig. 9). Staining pattern was cytoplasmic and paranuclear (Golgi pattern). Thirteen cases had weak (1+) expression (48%) and were distributed as follows based on molecular classification and pathology: 1 MB^{SHH} (D/N), 4 MB^{Grp3} (4/4 classic), 8 MB^{Grp4} (7/8 classic; 1/8 LC/A). Ten cases displayed moderate (2+) expression (37%), with 6 MB^{Grp4} (4/6 LC/A, 2/6 classic), 3 MB^{Grp3} (2/3 classic, 1/3 LC/A) and 1 MB^{WNT} (classic). Four cases displayed strong expression (15%), with 3 MB^{Grp3} (3/3 LC/A) and 1 MB^{SHH} (LC/A).

For further analyses, moderate and strong expression were joined in a moderate-strong expression group, featuring 14 cases (51.9%), and contrasted with the weak expression group.

Figure 9. Immunohistochemical expression of JAM-C

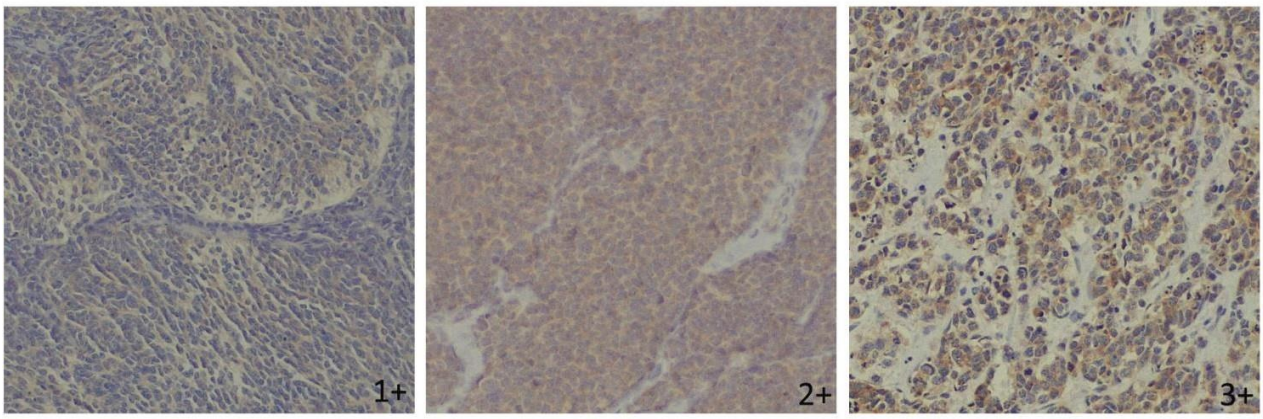

Figure 10. Comparison between gene expression and immunohistochemical expression of JAM-3/JAM-C

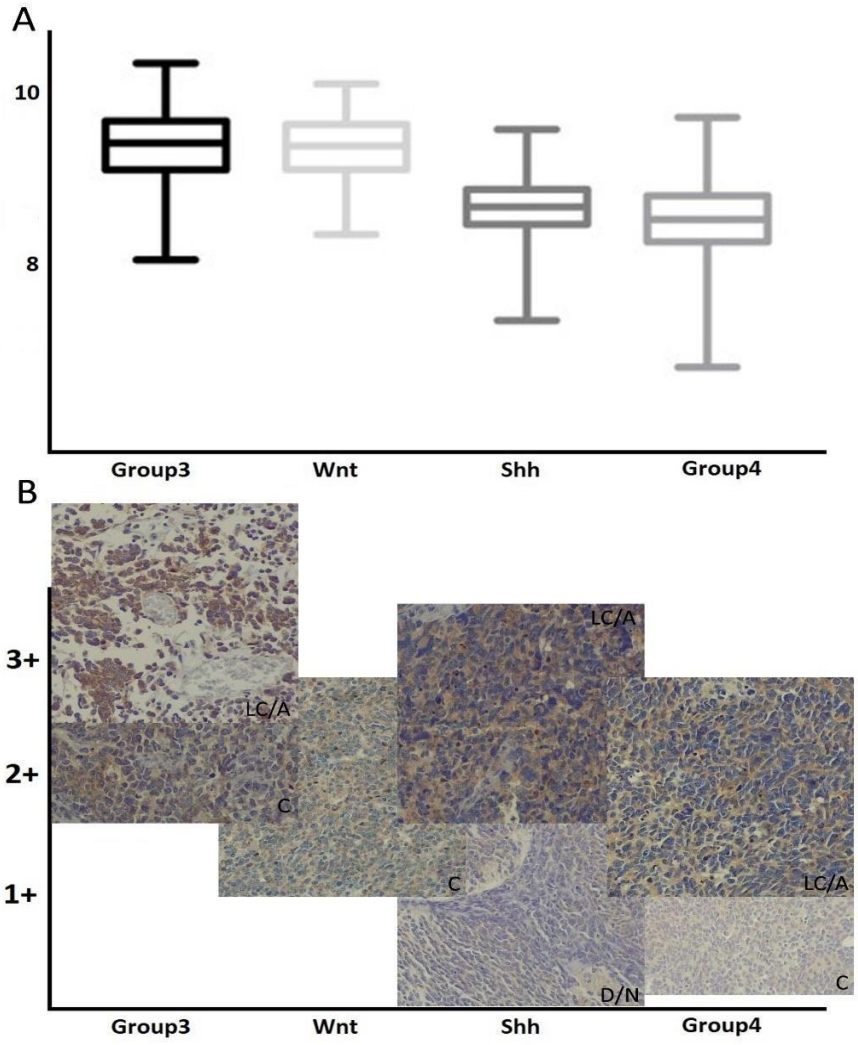

4.8 Associations between JAM-C expression and clinicopathological features

Table 7. Association between JAM-C expression and clinicopathological features

		% with moderate-high expression	*p*
Age	≤36m	75.0	0.32
	>36m	47.8	
Gender	F	58.8	0.35
	M	40.0	
Metastasis	no	50.0%	0.70
	yes	60.0%	
Histologic variant	Classic	35.3%	0.019 *
	DN	0%	
	LCA	88.9%	
Molecular subgroup	WNT [a]	50.0%	[a] 0.97; [b] 0.31
	SHH [a]	50.0%	
	Subgroup 3 [b]	55.6%	
	Subgroup 4 [b]	33.3%	

[a] classified by IHC; [b]classified by Nanostring

For 22 cases with follow up data, mean survival was 81.2 months (95%CI 56.2 – 106.2). Of these, only 9 had data on JAM-C expression and entered the following analysis. Those with moderate-high JAM-C expression (n=5) had a lower survival than those with low expression (n=4); however, the difference did not reach statistical significance (Log rank chi square=0.013, df=1, p=0.91) (Table 8, Figure 11).

Table 8 and Figure 11. Kaplan Meyer analysis: survival by JAM-C expression

JAM3_cat	Mean			
	Stima	Errore std.	95%CI	
			Lower	Upper
neg-low	97,203	26,860	44,558	149,849
mod-high	75,629	19,014	38,360	112,897
Global	86,022	18,399	49,960	122,084

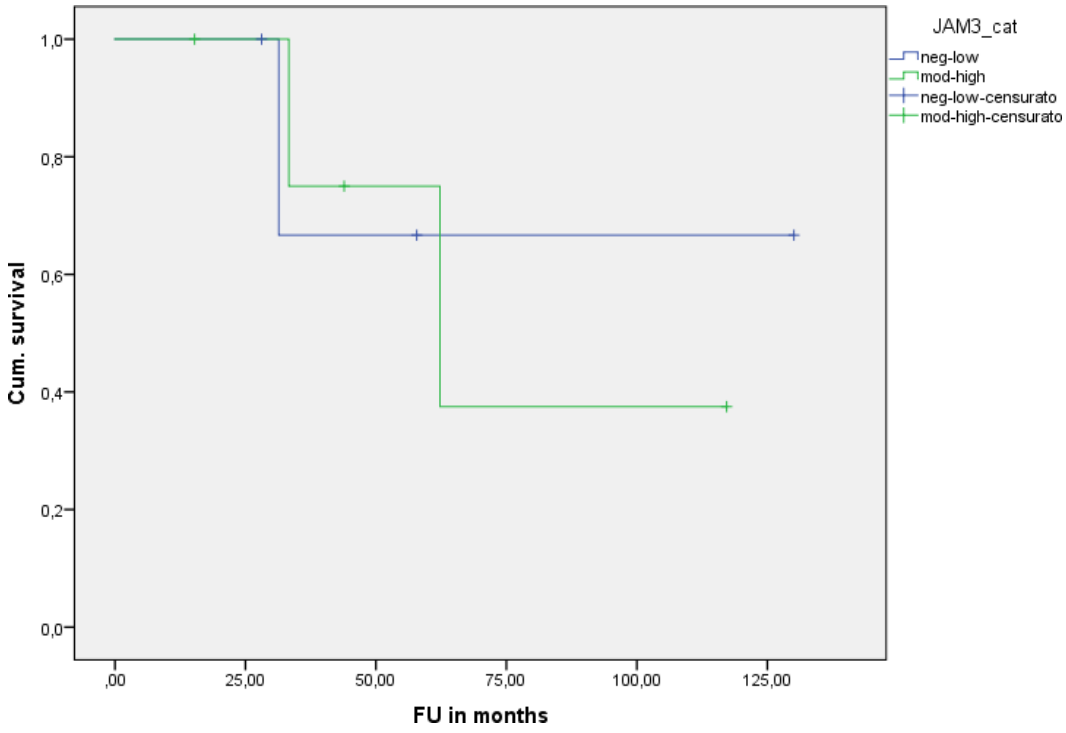

5. Discussion

In this study we investigated the expression of JAM molecules in MB based on two hypotheses. The first was that JAM-A could be upregulated in MB^{Grp3} since previous studies across different tumours demonstrated co-expression (as well as co-localization) of JAM-A and CD133, a well- known cancer stem-cell marker which is hyper-expressed in MB^{Grp3} [47,48]. The second relied on the observation that impaired migration of CGN precursors during CNS development contributes to the pathogenesis of MB, as recently documented both in cell cultures and animal models [29]. Based on this mechanism, we aimed to evaluate if JAM-B and JAM-C, which are critical for CGN migration, are deregulated across different subgroups of MB.

Analyses of gene expression data indicated that JAMs are differentially expressed across molecular subgroups of MB. Although we did not confirm our first hypothesis, we found that JAM3 can be useful in discriminating between MB^{Grp3} and MB^{Grp4}, with higher expression being associated with MB^{Grp3}, LC/A morphology and shorter survival. These findings were only partially supported by protein expression data, since high immunohistochemical expression (3+) of JAM-C was strongly associated with a subset of MB^{Grp3} with LC/A morphology but did not allow differentiation between consensus MB^{Grp3} and MB^{Grp4}. Furthermore, high to moderate immunohistochemical expression of JAM-C was significantly associated with LC/A morphology across different molecular subgroups. Finally, survival analyses displayed a trend for a shorter survival of patients with high expression of JAM-C. However, this finding did not reach significance, probably due to the small sample.

Our results indicate that concordance between transcriptional data and protein expression as detected by immunohistochemistry is incomplete. In line with this finding, a recent study focusing on correlation between mRNA and protein abundance in MB showed that only 45% of examined genes had a statistically significant correlation with protein levels [55]. Several factors have been shown to influence the gene/protein correlation, with the *biological function of the protein* being one of the most relevant. In this regard, cancer cells of MB have been shown to prioritize translation of genes belonging to metabolic and ribosomal pathways. This could explain why we did not find a full correspondence between the mRNA levels and protein expression in JAMs, which are mainly involved into other cellular functions (adhesion/migration/signalling).

The *half-life of mRNA and proteins* is also regarded as an important factor that influences mRNA/protein correlation, with stable molecules being associated with higher mRNA/protein correlation. Post-transcriptional regulation of JAMs has not been studied in detail, but growing evidence indicates that MicroRNA (miRNA) and processes like RNA editing are capable of controlling JAM's transcripts stability. For instance, miR-145, miR-495, and miR-34/449 have been shown to downregulate JAM-A expression levels in gliomas, whereas miR-146a leads to upregulation [30, 46]. Furthermore, hypoxia-induced RNA editing, which is associated with tumorigenesis, is known to stabilize JAM-A mRNA, thus resulting into higher levels of transcripts. Interestingly, a recent study demonstrated that in tumour cells hyper-edited mRNAs are often retained into specific nuclear compartments (paraspeckles) in order to prevent immediate translation, which can be promptly achieved in response to cellular stress [30]. To some extent, this observation might explain the discrepancy between mRNA and protein expression found for JAM-A in our series.

Additional mechanisms that might account for discordant mRNA/protein levels include post-translational modifications such as N-glycosylation/phosphorylation, ubiquitin-proteasome-mediated degradation and protein shedding from cell surface. However, their contribution to post-translational regulation of JAMs expression in tumour cells is still largely unknown.

The association of LC/A morphology and JAM-3/JAM-C upregulation was robust throughout transcriptomic and immunohistochemical data. This association was found across different consensus molecular subgroups, since we observed moderate (2+) IHC expression of JAM-C in cases of LC/A MB belonging to SHH and Group4 subgroups. However, the highest levels of JAM- 3/JAM-C expression were found among consensus MBGrp3 in both datasets (transcriptomic and immunohistochemical). The results of multivariate analyses after adjusting for histologic variant and molecular subgroup further supported the view that JAM-3 upregulation was closely related to LC/A morphology, but did not predict prognosis independently from histology. However, JAM-3 acquired some prognostic value independently from consensus molecular subgroup in a subset of cases carrying the highest mRNA levels; despite the small sample, immunohistochemistry seemed to recapitulate this observation. Therefore, it is possible that JAM-3 acquires prognostic value only in a subset of MB^{Grp3} with LC/A morphology.

Recent studies based on integrative analytic approaches to methylation and gene expression data across large samples showed that MB^{Grp3} and MB^{Grp4} exhibited significant molecular overlap that

precluded clear cut separation [56-58]. According to their results, consensus Group3 and Group4 should be better divided into 4 to 8 subtypes. Despite the lack of complete concordance, these reports unanimously disclosed the existence of a Group3 signature with poor prognosis harbouring MYC amplification. Schwalbe et al. found that MB^{Grp3} was split into high-risk and low- risk subgroups, with the first being characterized by lower age (<3 ys), LC/A pathology, MYC amplification, GFI1 mutations and a 5-years OS of 37% [95% CI 25–53] [56]. Analyses from Cavalli et al. highlighted 3 subtypes emerging from consensus Group3, with group 3γ showing the worst prognosis compared to groups 3α and 3β, as well as enrichment of i17q and MYC copy number [57]. Finally, Lastowska et al. recognized three transcriptional subgroups resulting from consensus $MB^{non\text{-}WNT/SHH}$: Group3, Group4 and Intermediate 3-4 Group; according to their findings, Group3 displayed poor prognosis, metastasis at presentation, LC/A pathology and MYC amplification [58]. Our results are in coincidence with these findings: indeed, JAM-C expression does not separate consensus MB^{Grp3} and MB^{Grp4} but leads to identify a subset of MB^{Grp3} with LC/A pathology carrying poor outcomes which could at least partially correspond to such emerging high-risk subtype of MB^{Grp3}.

To our knowledge, this is the first study to investigate the role of JAM molecules in MB, both in terms of gene and protein expression. However, this study has limitations that need to be taken in account before interpreting these findings. First, data of gene and immunohistochemical expression were obtained from different samples, the latter being limited in size. Second, molecular subgrouping was assessed using Nanostring rather than a methylation arrays which may have been more accurate. Third, follow-up data were available only for a subset of cases with known immunohistochemical expression of JAM-C. Fourth, important informations such as MYC status were unavailable in the experimental cohort which precluded the full validation of our hypotheses.

In conclusion, JAM-C may have a role as subtyping marker and prognostic factor in pediatric MB. Further, our findings are consistent with recent evidence suggesting the need for a revision of consensus molecular subgroups, in particular MB^{Grp3} and MB^{Grp4}. Given the lack of reliable immunohistochemical markers for the emerging high-risk subgroup of MB^{Grp3}, with the exception of the recently described PDC protein [58], further studies should investigate the role of JAM- 3/JAM-C in relation to clinicopathological features, molecular characteristics (including MYC amplification) and overall prognosis.

References

[1] Louis DN, Perry A, Reifenberger G, et al. The 2016 World HealthOrganization Classification of Tumours of the Central NervousSystem: a summary. Acta Neuropathol. 2016; 131: 803–20.

[2] Smoll NR, Drummond KJ. The incidence of medulloblastomas and primitive neurectodermal tumours in adults and children. J Clin Neurosci. 2012; 19: 1541–44.

[3] Rutkowski S, von Hoff K, Emser A, et al. Survival and prognostic factors of early childhood medulloblastoma: an international metaanalysis. J Clin Oncol. 2010; 28: 4961-4968.

[4] Ostrom QT, Gittleman H, Fulop J, et al. CBTRUS statistical report: primary brain and central nervous system tumors diagnosed in the United States in 2008-2012. Neuro Oncol. 2015; 17(suppl 4): iv1-iv62.

[5] Sengupta S, Pomeranz Krummel D, Pomeroy S. The evolution of medulloblastoma therapy to personalized medicine. F1000Res. 2017; Apr 13;6:490.

[6] Taylor MD, Northcott PA, Korshunov A, et al. Molecular subgroups of medulloblastoma: the current consensus. Acta Neuropathol. 2012; 123:465-472. 24.

[7] Northcott PA, Dubuc AM, Pfister S, et al. Molecular subgroups of medulloblastoma. Expert Rev Neurother. 2012; 12:871-884.

[8] Jones DT, Jaeger N, Kool M, et al. Dissecting the genomic complexity underlying medulloblastoma. Nature. 2012; 488:100-105.

[9] Pugh TJ, Weeraratne SD, Archer TC, et al. Medulloblastoma exome sequencing uncovers subtype-specific somatic mutations. Nature. 2012; 488:106-110.

[10] Rausch T, Jones DT, Zapatka M, et al. Genome sequencing of pediatric medulloblastoma links catastrophic DNA rearrangements with TP53 mutations. Cell. 2012; 148:59-71.

[11] Robinson G, Parker M, Kranenburg TA, et al. Novel mutations target distinct subgroups of medulloblastoma. Nature. 2012; 488:43-48.

[12] Northcott PA, et al. Multiple recurrent genetic events converge on control of histone lysine methylation in medulloblastoma. Nat Genet. 2009; 41:465-472.

[13] Kool M, Korshunov A, Remke M, et al. Molecular subgroups of medulloblastoma: an international meta-analysis of transcriptome, genetic aberrations, and clinical data of WNT, SHH, Group 3, and Group 4 medulloblastomas. Acta Neuropathol. 2012; 123: 473–84.

[14] Cho YJ, Tsherniak A, Tamayo P, et al.: Integrative genomic analysis of medulloblastoma identifies a molecular subgroup that drives poor clinical outcome. J Clin Oncol. 2011; 29(11): 1424–30.

[15] Northcott PA, Shih DJ, Peacock J, et al.: Subgroup-specific structural variation across 1,000 medulloblastoma genomes. Nature. 2012; 488(7409): 49–56.

[16] MacDonald TJ, Packer RJ: Pediatric Medulloblastoma. Medscape Drugs & Diseases. 2014.

[17] Lin CY, Erkek S, Tong Y, et al.: Active medulloblastoma enhancers reveal subgroup-specific cellular origins. Nature. 2016; 530(7588): 57–62.

[18] Shih DJ, Northcott PA, Remke M, et al.: Cytogenetic prognostication within medulloblastoma subgroups. J Clin Oncol. 2014; 32(9): 886–96.

[19] Northcott AP, Korshunov A, Witt H, et al. Medulloblastoma comprises four distinct molecular variants. J Clin Oncol. 2011; 29:1408–1414.

[20] Northcott PA, Shih DJH, Remke M, et al. Rapid, reliable, and reproducible molecular sub-grouping of clinical medulloblastoma samples. Acta Neuropathol. 2012; 123:615–626.

[21] Schwalbe EC, Williamson D, Lindsey JC, et al. DNA methylation profiling ofmedulloblastoma allows robust subclassification and improved outcome prediction using formalin-fixed biopsies. Acta Neuropathol. 2013; 125:359–371.

[22] Ellison DW, Dalton J, Kocak M, et al. Medulloblastoma: clinicopathological correlates of SHH, WNT, and non-SHH/WNT molecular subgroups. ActaNeuropathol. 2011; 121:381–396.

[23] Min HS, Lee JY, Kim SK, et al. Genetic grouping of medulloblastomas by representative markers in pathologic diagnosis. Transl Oncol. 2013; 6:265–272.

[24] Kaur K, Kakkar A, Kumar A, et al. Integrating Molecular Subclassification of Medulloblastomas into Routine Clinical Practice: A Simplified Approach. Brain Pathol. 2016; May;26(3):334-43.

[25] Palma V, Lim DA, Dahmane N, et al. Sonic hedgehog controls stem cell behavior in the postnatal and adult brain. Development 2005; 132:335–344.

[26] Schüller U, Heine VM, Mao J, et al. Acquisition of granule neuron precursor identity is a critical determinant of progenitor cell competence to form Shh-induced medulloblastoma. Cancer Cell. 2008; 14,123–134.

[27] Farioli-Vecchioli S, Cinà I, Ceccarelli M, et al. Tis21 knock-out enhances the frequency of medulloblastoma in Patched1 heterozygous mice by inhibiting the Cxcl3-dependent migration of cerebellar neurons. J Neurosci. 2012; 32, 15547–15564.

[28] Haag D, Zipper P, Westrich V, et al. Nos2 inactivation promotes the development of medulloblastoma in Ptch1(+/−) mice by deregulation of Gap43-dependent granule cell precursor migration. PLoS Genet. 2012;8:e1002572.

[29] Ceccarelli M, Micheli L, Tirone F. Suppression of Medulloblastoma Lesions by Forced Migration of Preneoplastic Precursor Cells with Intracerebellar Administration of the Chemokine Cxcl3. Front Pharmacol. 2016; Dec 16;7:484.

[30] Ebnet, K. Junctional adhesion molecules (jams): Cell adhesion receptors with pleiotropic functions in cell physiology and development. Physiological reviews. 2017; 97(4), 1529-1554.

[31] Kostrewa D, Brockhaus M, D'Arcy A, et al. X-ray structure of junctional adhesion molecule: structural basis for homophilic adhesion via a novel dimerization motif. EMBO J. 2001; 20: 4391–4398.

[32] Mandicourt G, Iden S, Ebnet K, et al.. JAM-C regulates tight junctions and integrin-mediated cell adhesion and migration. J Biol Chem. 2007; 282: 1830– 1837.

[33] Peddibhotla SS, Brinkmann BF, Kummer D, et al. Tetraspanin CD9 links junctional adhesion molecule-A to v 3 integrin to mediate basic fibroblast growth factor-specific angiogenic signaling. Mol Biol Cell. 2013; 24: 933–944.

[34] Stelzer S, Ebnet K, Schwamborn JC. JAM-A is a novel surface marker for NG2-glia in the adult mouse brain. BMC Neurosci. 2010; 11: 27.

[35] Famulski JK, Trivedi N, Howell D, et al. Siah regulation of Pard3A controls neuronal cell adhesion during germinal zone exit. Science. 2010; 330: 1834–1838, 2010.

[36] Solimando AG, Brandl A, Mattenheimer K, et al. JAM-A as a prognostic factor and new therapeutic target in multiple myeloma. Leukemia. 2018; Mar;32(3):736-743.

[37] Xu PP, Sun YF, Fang Y, et al. JAM-A overexpression is related to disease progression in diffuse large B-cell lymphoma and downregulated by lenalidomide. Sci Rep. 2017; Aug 7;7(1):7433.

[38] Zhang M, Luo W, Huang B, et al. Overexpression of JAM-A in non-small cell lung cancer correlates with tumor progression. PloS ONE. 2013; 8(11):e79173.

[39] Tian Y, Tian Y, Zhang W, et al. Junctional adhesion molecule-A, an epithelial-mesenchymal transition inducer, correlates with metastasis and poor prognosis in human nasopharyngeal cancer. Carcinogenesis. 2015; 36(1):41–48.

[40] Fong D, Spizzo G, Mitterer M, et al. Low expression of junctional adhesion molecule A is associated with metastasis and poor survival in pancreatic cancer. Ann Surg Oncol. 2012; 19(13):4330–4336.

[41] Gutwein P, Schramme A, Voss B, et al. Downregulation of junctional adhesion molecule-A is involved in the progression of clear cell renal cell carcinoma. Biochem Biophys Res Commun. 2009; 380(2):387–391.

[42] Huang JY, Xu YY, Sun Z, et al. Low junctional adhesion molecule A expression correlates with poor prognosis in gastric cancer. J Surg Res. 2014; 192(2):494–502.

[43] McSherry EA, McGee SF, Jirstrom K, et al. JAM-A expression positively correlates with poor prognosis in breast cancer patients. Int J Cancer. 2009; 125(6):1343–1351.

[44] Naik MU, Naik TU, Suckow AT, at al. Attenuation of junctional adhesion molecule-A is a contributing factor for breast cancer cell invasion. Cancer Res. 2008; 68(7):2194–2203.

[45] Thiagarajan PS, Hitomi M, Hale JS, et al. Development of a fluorescent reporter system to delineate cancer stem cells in triple-negative breast cancer. Stem Cells. 2015: 33(7):2114–2125.

[46] Rosager AM, Sørensen MD, Dahlrot RH, et al. Expression and prognostic value of JAM-A in gliomas. J Neurooncol. 2017; Oct;135(1):107-117.

[47] Raso A, Mascelli S, Biassoni R, et al. High levels of PROM1 (CD133) transcript are a potential predictor of poor prognosis in medulloblastoma. Neuro-oncology. 2011; 13(5), 500-508.

[48] Garg N, Bakhshinyan D, Venugopal C, et al. CD133+ brain tumor-initiating cells are dependent on STAT3 signaling to drive medulloblastoma recurrence. Oncogene. 2017; 36(5), 606.

[49] De Grandis M, Mancini SJ, Vey N, et alJAM-C Expression as a Biomarker to Predict Outcome of Patients with Acute Myeloid Leukemia—Response. Cancer research. 2018; 78(21), 6342-6343.

[50] Tenan M, Aurrand-Lions M, Widmer V, et al. Cooperative expression of junctional adhesion molecule-C and-B supports growth and invasion of glioma. Glia. 2010; 58(5), 524-537.

[51] Ghislin S, Obino D, Middendorp S, et al. Junctional adhesion molecules are required for melanoma cell lines transendothelial migration in vitro. Pigment cell & melanoma research. 2011; 24(3), 504-511.

[52] Hao S, Yang Y, Liu Y, et al. JAM-C promotes lymphangiogenesis and nodal metastasis in non-small cell lung cancer. Tumor Biology. 2014; 35(6), 5675-5687.

[53] Garrido-Urbani S, Vonlaufen A, Stalin J, et al. Junctional adhesion molecule C (JAM-C) dimerization aids cancer cell migration and metastasis. Biochimica et Biophysica Acta (BBA)-Molecular Cell Research. 2018; 1865(4), 638-649.

[54] Thompson EM, Hielscher T, Bouffet E, et al. Prognostic value of medulloblastoma extent of resection after accounting for molecular subgroup: a retrospective integrated clinical and molecular analysis. The Lancet Oncology. 2016; 17(4), 484-495.

[55] Rivero-Hinojosa S, Lau LS, Stampar M, et al. Proteomic analysis of Medulloblastoma reveals functional biology with translational potential. Acta Neuropathol Commun. 2018; Jun 7;6(1):48.

[56] Schwalbe EC, Lindsey JC, Nakjang S, et al. Novel molecular subgroups for clinical classification and outcome prediction in childhood medulloblastoma: a cohort study. Lancet Oncol. 2017; Jul;18(7):958-971.

[57] Cavalli FMG, Remke M, Rampasek L, et al. Intertumoral Heterogeneity within Medulloblastoma Subgroups. Cancer Cell. 2017; Jun 12;31(6):737-754.e6.

[58] Łastowska M, Trubicka J, Niemira M, et al. Medulloblastoma with transitional features between Group 3 and Group 4 is associated with good prognosis. J Neurooncol. 2018; Jun;138(2):231-240.